

# Biomechanics of Traumatic Brain Injury

Tanu Khanuja

A Dissertation Submitted to  
Indian Institute of Technology Hyderabad  
In Partial Fulfillment of the Requirements for  
The Degree of Master of Technology



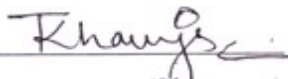
भारतीय प्रौद्योगिकी संस्थान हैदराबाद  
Indian Institute of Technology Hyderabad

Department of Biomedical Engineering

June, 2014

## **Declaration**

I declare that this written submission represents my ideas in my own words, and where others' ideas or words have been included, I have adequately cited and referenced the original sources. I also declare that I have adhered to all principles of academic honesty and integrity and have not misrepresented or fabricated or falsified any idea/data/fact/source in my submission. I understand that any violation of the above will be a cause for disciplinary action by the Institute and can also evoke penal action from the sources that have thus not been properly cited, or from whom proper permission has not been taken when needed.

  
\_\_\_\_\_  
(Signature)

**Tanu Khanuja**

BM12M1004

# Approval Sheet

This thesis entitled Biomechanics of Traumatic Brain Injury by Tanu Khanuja is approved for the degree of Master of Technology from IIT Hyderabad.



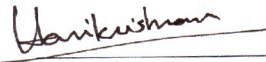
**Dr. Renu John**

Assistant professor  
Department of Biomedical Engineering  
Indian Institute of Technology Hyderabad  
Examiner



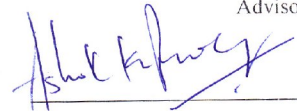
**Dr. Subha Narayan Rath**

Assistant professor  
Department of Biomedical Engineering  
Indian Institute of Technology Hyderabad  
Examiner



**Dr. Harikrishnan Narayanan Unni**

Assistant professor  
Department of Biomedical Engineering  
Indian Institute of Technology Hyderabad  
Advisor



**Dr. Ashok Kumar Pandey**

Assistance Professor  
Department of Mechanical Engineering  
Indian Institute of Technology Hyderabad  
Chairman

## **Acknowledgements**

Sincere gratitude to my supervisor, Dr. Harikrishnan Narayanan Unni, who really is a source of optimism, encouragement, fruitful ideas and support. I want to thank Dr. Renu John and Dr. Subha Narayan Rath for giving their valuable time. In addition my acknowledgments go to Mr. Madhu for helping with installation of ANSYS software in Kandi lab. I express my gratitude to all the supportive colleagues in the Department who have greatly facilitated my work. I am thankful to Narendra and Hanu for helping me to learn MATLAB and Manish for encouraging me always. And I am very thankful to my family for always being with me. Thank you all!

Dedicated to

My Father

## **Abstract**

This project is aimed to generate a 2D model of head to study biomechanics of head injuries due to external forces acting in different direction. The purpose of this work is the development of a 2D finite element model (FEM), using equations of elasticity and viscoelasticity to model the stress-strain distribution in the head due to external impacts. A variational constitutive model for soft biological tissues such as brain is utilized to reproduce axonal damage and cavitation injury through inelastic deformation and with the constitutive model for hard tissues such as brain possessing elastic properties. A constitutive model for these biological tissues is formulated with a finite strain regime. Most of the physiological damage to living tissues are caused by relative motions within the tissues (e.g. in head injury, due to relative motion between brain and skull), due to tensile and shearing structural failures. The Model includes skull, brain and CSF as major components so material response is split into elastic and viscoelastic components, including rate effects, shear and porous plasticity and finite viscoelasticity. To describe biological soft tissues such as brain tissue a viscoelastic material model is employed and to describe skull and cerebrospinal fluid we are an elastic model is employed. Skull is considered to be transverse isotropic. The present FEM simulation focuses on brain injuries from static and dynamic loading resulting from frontal, top, back and oblique head impacts and prediction of localization, extension, and intensity of tissue damage. In the present work, brain 2D geometry is generated from MRI of adult head. We intend to obtain insight into the severity of brain injury by modeling by analyzing the stress-strain pattern under static and dynamic loading.

## **Nomenclature**

TBI – Traumatic Brain Injury

DAI – Diffuse Axonal Injury

EDH - Epidural Hematoma

SDH – Subdural Hematoma

MRI – Magnetic Resonance Imaging

CT – Computed Tomography

SCI – Spinal Cord Injury

FEM – Finite Element Modeling

## List of Figures

Figure 1-1: MRI of sagittal section of human head .....	4
Figure 1-2: Layers in coronal section of human head .....	5
Figure 1-3: Biomechanics of Subdural hematoma .....	8
Figure 1-4: CT of Epidural Hematoma .....	9
Figure 1-5: Biomechanics of Contusion.....	9
Figure 1-6: Biomechanics of Concussion .....	11
Figure 2-1: MRI and Edge detected signal using MATLAB .....	14
Figure 2-2: Line Model drawn using B-spline with loading directions .....	15
Figure 2-3: Flow Chart of Finite Element Modeling .....	16
Figure 2-4: Plane 183 node element.....	17
Figure 2-5: Displacement with No. of elements 3642 .....	18
Figure 2-6: Displacement with No. of elements 33272 .....	18
Figure 2-7: Displacement with No. of elements 106169 .....	18
Figure 2-8: Displacement with No. of elements 205411 .....	19
Figure 2-9: Skull bone representation .....	21
Figure 3-1: Frontal Loading Point.....	26
Figure 3-2: Boundary condition for static load .....	26
Figure 3-3: Shear strain contour for point load.....	27
Figure 3-4: Shear strain contour for distributed load .....	27
Figure 3-5: Top Loading Point.....	28
Figure 3-6: Shear strain contour for top point load.....	28
Figure 3-7: Shear strain contour for top distributed load .....	28
Figure 3-8: Boundary condition for Dynamic (a) Frontal and Back loading (Displacement and rotation along Y direction is zero) (b) Top loading (Displacement and rotation along X direction is zero).....	29
Figure 3-9: Dynamic frontal loading - Shear stress contours.....	31
Figure 3-10: Shear stress at coup site vs. time .....	32
Figure 3-11: Shear stress at contre-coup site vs. time .....	32
Figure 3-12: Dynamic Frontal loading- shear strain vs. time contours.....	33



Figure 3-13: Dynamic top loading - shear stress vs. time contours .....	34
Figure 3-14: Dynamic top loading - shear strain vs. time contours .....	35
Figure 3-15: Dynamic back loading - Shear stress vs. time contours .....	36
Figure 3-16: Dynamic back loading - Shear strain vs. time contours .....	37

## List of Tables

Table 1-1: Classification of TBI based on severity.....	7
Table 2-1: Parameters for constitutive model of skull bone .....	21
Table 2-2: Material Properties of CSF .....	22
Table 2-3: Material properties for CNS .....	24

# Contents

Declaration.....	ii
Approval Sheet .....	iii
Acknowledgements.....	iv
Abstract.....	vi
<b>Nomenclature .....</b>	<b>vii</b>
<b>1 Introduction.....</b>	<b>1</b>
1.1 Thesis Overview .....	1
1.2 Literature Review .....	2
1.3 Aim of Project.....	3
1.4 Anatomy of Human Head.....	3
1.4.1 Skull .....	4
1.4.2 Cerebrospinal fluid.....	4
1.4.3 Meninges .....	5
1.4.4 Central Nervous System (CNS) .....	6
1.5 Traumatic Brain Injury .....	6
1.5.1 Focal Injury .....	7
1.5.1.1 Subdural Hematoma(SDH) .....	8
1.5.1.2 Epidural Hematoma(EDH) .....	9
1.5.1.3 Intracerebral Hematoma (ICH) .....	9
1.5.1.4 Contusion .....	9
1.5.2 Diffuse Injury .....	10
1.5.2.1 Concussion.....	10
1.5.2.2 Diffuse Axonal Injury .....	11
<b>2 Model Development.....</b>	<b>13</b>
2.1 Introduction to MRI.....	13
2.2 Image Processing in MATLAB .....	14
2.3 Finite Element Model Generation.....	15
2.3.1 Mesh Generation and Optimization.....	16
2.4 Material Properties.....	19
2.4.1 Skull .....	19
2.4.2 CSF.....	22

2.4.3	Brain .....	23
2.5	Boundary Conditions .....	24
<b>3</b>	<b>Results and Discussion .....</b>	<b>25</b>
3.1	Static Loading .....	26
3.1.1	Frontal Loading .....	26
3.1.2	Top Loading .....	28
3.2	Dynamic Loading .....	29
3.2.1	Frontal Loading .....	29
3.2.2	Top Loading .....	33
3.2.3	Back Loading .....	35
<b>4</b>	<b>Conclusion and Future Work .....</b>	<b>38</b>
4.1	Conclusion .....	38
4.2	Future Work.....	38
<b>References</b> .....		<b>40</b>

# Chapter 1

## Introduction

The head is known as the body part which injures frequently during various accidents and may cause severe life threatening injuries. The head region is considered to be the most critical body region in crash situations because of the injuries to the central nervous system which are irreversible. It is not yet completely understood in which way an external mechanical load, applied on the human head, leads to head and brain injury. For finding the reason behind this, we must understand the key phenomena occur during these impacts to the brain. The key-problem here is that, one cannot record in-vivo brain response during injury and therefore, numerical models of the human head under impact conditions are developed. For developing a numerical model one requires knowledge of the constitutive behavior of human brain tissue and information on relevant dynamical phenomena during impact situations like shear stress, shear strain, pressure and wave propagation. Mimicking the constitutive behavior of brain tissue can be realized by the use of model materials. On the other hand, a model material can be applied in an experimental validation of a numerical model. A finite element model of human head can be established to be able to determine the cause of the head trauma during various impacts with sufficient accuracy. A model of the head can be constructed from the patient specific Magnetic Resonance Imaging (MRI) images and used to simulate the head trauma. By simulating head trauma, one may be able to obtain the fracture propagation of the skull. Biomechanical studies of this kind can also help to determine the injury mechanism of skull bones from different impact scenarios.

### 1.1 Thesis Overview

The thesis covers the whole process of simulating human head trauma from various accidents. MRI image (sagittal) data of an adult head is employed to generate a 2D model of the head. The image data is processed to obtain the complex geometry of skull, cerebrospinal fluid and brain and further processed to construct a triangular and quadrilateral mesh in ANSYS, resulting in a model suitable for FE simulation. The meshed model is solved using ANSYS to compute the stress-strain distribution in skull, cerebrospinal fluid (CSF) and brain due to the impact of static and dynamic type. Results

from an impact to the frontal, top and back of the head are analyzed. Comparison of the model can be done with injury pattern from the various impacts against published injury patterns of post mortem human subject (PMHS) studies<sup>1</sup>.

The thesis material is organized as follows. Chapter 1.2 covers previous studies found in literature relevant for the background of this study. Chapter 1.3 goes through the aim of the project and chapter 1.4 covers the anatomy of the human skull, CSF, Meninges and central nervous system. Chapter 2 covers the Model construction from the MRI image. 2.1 goes through the introduction of MRI. 2.2 explain how the 2D geometry is constructed and how the mesh optimization is obtained to increase accuracy of the model. Chapter 3 depicts results from impact simulations; Chapter 4 includes conclusion and future work of the model.

## **1.2 Literature Review**

A major part of the reported literature is concerned with two dimensional models representing a sagittal section of the human or animal head. A Finite element idealization of the mid sagittal section of a human brain was constructed from a photograph by Melvin et.al<sup>2</sup>. Using this model, consisting of a rigid skull and a homogeneous brain, Hybrid III sled tests were simulated using experimental acceleration-time histories of the centre of gravity of the dummy head as input. The relative severity of the tests as judged by the HIC appeared to be opposite to that judged on the basis of either calculated maximum pressures or calculated maximum shear stresses. This model was also employed in Rhesus monkey based study to illustrate the application of a scaling law. Employing the same model serving as a starting point, Trosseille<sup>3</sup> carried out a parametric study to compare trends in simulation results with those of human cadaver experiments. They extended the original model with an 'extremely rigid' beam representing the tentorium cerebella. Furthermore the influence of the no-slip condition at the skull-brain interface was observed to be diminished by incorporating a layer with a low shear modulus to model the cerebrospinal fluid (CSF) surrounding the brain. A model of a para-sagittal section of an average human head was developed by Chu and Lee<sup>4</sup> to study mechanism of cerebral contusions with spectral attention for coup - contre-coup phenomena. Validation against Nahum<sup>1</sup> experiments showed the calculated pressures to be roughly consistent with, but lower than, the experimental data. For frontal and occipital impacts almost identical tensile stresses were found in the contre-coup regions. Ruan et.al<sup>5</sup> conducted a study of the side impact response using coronal-plane models of a 50<sup>th</sup> percentile human head. They concluded that it is

improper to validate FE models based on pressure calculations and then use them for injury prediction. This is apparent since tissue level models<sup>6</sup> have shown that diffuse axonal injury (DAI) is a function of strain and not pressure. The more relevant parameter for validation of a FE model of the human head should therefore be strain. Such strain data do not exist, however, relative displacement data between the brain and skull are available, and therefore provide a means of model validation of localized brain motion that is more comprehensive than pressure data. The first relative motion recorded during human cadaver head impacts in anatomical coordinate components was provided by Al-Bsharat et.al<sup>7</sup>. The first relative motion recorded during human cadaver head impacts in anatomical coordinate components was provided.

In the present model of human head, mechanical properties of skull, CSF and brain tissue are obtained from literature<sup>8</sup>. It has been shown that brain tissue behaves like a nonlinear visco-elastic material. It is described in detail in Chapter 2.

### **1.3 Aim of Project**

This study primarily focuses on the development of a 2D FE model of the Human Head. The present thesis includes:

- The development of a 2D Finite Element (FE) model of the human head.
- Parametric studies of the influences of static and dynamic loading on the head.
- Evaluation of the shear stress and strain to a variation of impact direction to the human head, and its consequences for injury prediction.
- Coup and contre-coup injuries prediction with respect to sinusoidal loading with different frequencies.

### **1.4 Anatomy of Human Head**

Different tissue layers such as the scalp, skull bone, Dural, arachnoidal and pial membranes as well as cerebrospinal fluid (CSF) cover the brain see Fig 1.1. The skull bone can be viewed as a three-layered sandwich structure with an inner and outer table of compact bone and a diploe of spongy bone sandwiched between them as a core<sup>9</sup>. The lower separating membrane, the tentorium cerebelli, resides on the inferior wall of the skull, and separates the cerebrum from the cerebellum and brain stem. The brain, with its covering membranes and

CSF, is connected to the spinal cord through the foramen magnum. The inferior part of the skull base is attached to the neck by articulation through ligaments and muscles.

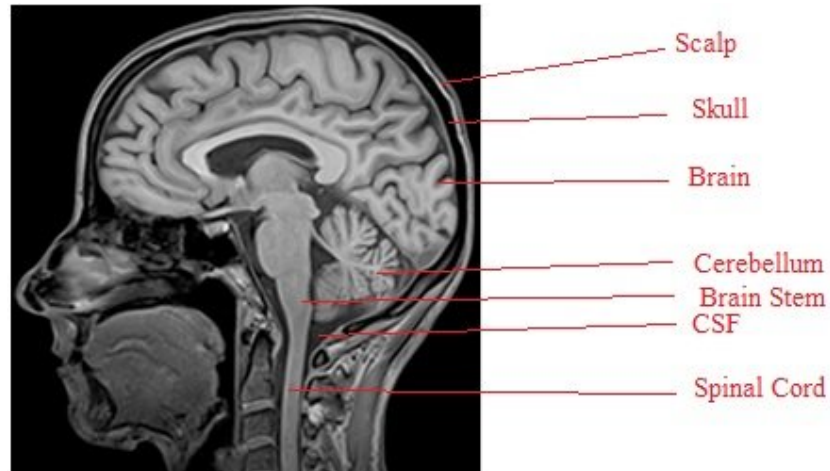


**Figure 1-1: MRI of sagittal section of human head**<sup>10</sup>[MRI Image source]

#### **1.4.1 Skull**

The thickness of the skull varies between 4 and 7 mm<sup>11</sup>. The base of the braincase is an irregular plate of bone containing depressions and ridges plus small holes (foramen) for arteries, veins, and nerves, as well as the large hole (the foramen magnum) that is the transition area between the spinal cord and the brainstem. The bones of the cranium are connected at lines called sutures. The skull, or cranium, protects the brain and the organs of special sensation, allows the passage of air and food, and supports the teeth. It consists of a series of bones, mostly united at immovable joints. The mandible, however, can move freely at a synovial articulation. Some bones of the skull are paired, whereas others are not. Each consists of external and internal tables of compact bone and a middle spongy layer, the diploe. The inner and outer layer of compact bone in the skull can (unlike the long bones) be considered to be isotropic in the tangential direction of the skull bone (transversely isotropic). The skull is covered by periosteum and lined by Dura (endocranium).

#### **1.4.2 Cerebrospinal fluid**

The brain and spinal cord are surrounded by CSF. Average CSF thickness ranges from 0.25-5mm. It is thought to have a mechanical protective function for the brain. In case of a mechanical load applied to the head, it allows the brain to move independently to the cranium to some extent. Furthermore, it provides a stable internal environment, which is



necessary for normal brain functioning. Its total volume is approximately 150 ml, of which 25 ml is situated within four communicating ventricles inside the brain. The remaining part is located inside the subarachnoid space. It is composed of 99% water and is similar in composition to blood plasma, from which it originates. Fluid fills the entire subarachnoid space and surrounds the brain with a protective cushion that absorbs shock waves to the head<sup>12</sup>. As a further means of protection, there are fibrous filaments known as arachnoid trabeculations, which extend from the arachnoid to the pia and help “anchor” the brain to prevent it from excessive movement in cases of sudden acceleration or deceleration.

### 1.4.3 Meninges

The meninges consist primarily of connective tissue, and they also form part of the walls of blood vessels and the sheaths of nerves as they enter the brain and as they emerge from the skull. The meninges consist of three layers: the dura mater, the arachnoid, and the pia mater. Brain tissue, having the consistency of a heavy pudding, is the most delicate of all body tissues. For protection, this vital organ is located in a sealed bony chamber, the skull. To protect it further from the rough bone and from blows and shocks to the head, the brain is enveloped by the meninges. The outermost dura mater is adherent or close to the inner surface of the bone. Beneath the dura mater is the middle covering, the thin and fibrous arachnoid. The third and innermost layer is the very thin, delicate, and capillary-rich pia mater, which is intimately attached to the brain and dips down into the sulci and fissures. The dura mater is the strongest meninx with thickness in the range of 0.3-0.8mm and it is attached to the inside of the cranium.

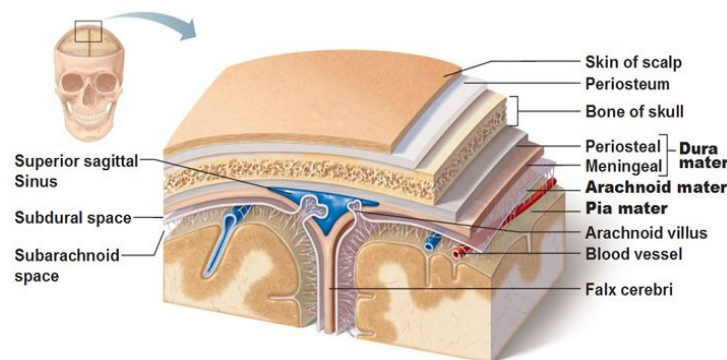


Figure 1-2: Layers in coronal section of human head<sup>13</sup>

The arachnoid is a thin meningeal layer lying intermediate between the other two meninges. Its function is to insulate the central nervous system (CNS) from the rest of the body. It is attached to the dura Mater. The pia mater also is a thin meningeal layer and it is attached to the surface of the CNS, which means that it follows the irregularities of the surface of the CNS<sup>14</sup>.

#### **1.4.4 Central Nervous System (CNS)**

The nervous system of vertebrates is divided into the central nervous system (CNS) and the peripheral nervous system. The CNS consists of the brain and the spinal cord. It is covered by the meninges to provide protection. Further protection is given by the cranium, i.e. the part of the skull holding the brain, and by the vertebrae. The brain consists of the Cerebrum, the cerebellum, and the brain stem. The latter is connected to the spinal cord. The cerebrum accounts for about 83% of the total brain mass and it consists of the two cerebral hemispheres. The exterior of the cerebrum consists of the cerebral cortex. It contains gray matter and is 2 to 5 mm in thickness. Inferior to the cerebral cortex lies the cerebral white matter. Gray matter is composed primarily of nerve-cell bodies concentrated in locations on the surface of the brain and deep within the brain. White matter is composed of myelinated (myelin is a soft, white somewhat fatty material) axons that largely form tracts to connect parts of the CNS to each other. At a microscopic level, CNS is primarily a network of neurons and supportive tissue functionally arranged into areas that are gray or white in color. Brain tissue can be likened to a soft gel because of the high water content (about 80 %), and it can be considered nearly incompressible. This observation is confirmed by reported values of the bulk modulus for brain tissue of about  $K=2.1$  GPa, which is roughly 105 times larger than the shear modulus. Therefore, the deformation of brain tissue can be assumed to depend on the shear modulus only. Most of the testing of brain tissue has therefore been performed in shear or torsion<sup>15</sup>.

### **1.5 Traumatic Brain Injury**

Traumatic brain injury (TBI) is damage to the brain caused by a blow to the head. The severity of the injury may range from minor, with few or no lasting consequences, to major, resulting in profound disability or death. Although any injury to the brain is serious, and severe damage can be fatal, medical and surgical advances have improved the odds for surviving a TBI. TBIs are classified according to the severity and mechanism of injury as depicted in Table 1.1:

Table 1-1: Classification of TBI based on severity<sup>17</sup>

<b>Injury Severity</b>	<b>Loss of Consciousness (LOC)/Coma duration</b>	<b>Signs</b>	<b>Symptoms</b>
Mild	LOC for less than 30 minutes or no LOC may cause.	Loss of memory may occur for less than 24 hrs, with temporary or permanent mental state.	Symptoms after concussion can be seen.
Moderate	Patient may go to coma for more than 20-30 minutes but less than 24 hrs	Bruising and bleeding in the brain, which can be observed in CT and MRI scans.	Some long term problem in one or more areas of life.
Severe	Coma for more than a day or a week.	Skull fractures / bruising and bleeding, which can be observed in CT and MRI scans	Long term impairments in one or more areas of life

Clinically brain injuries can be classified in two broad categories: focal injuries and diffuse injuries<sup>16</sup>. The focal brain injury is a lesion causing local damage which can be seen by the naked eye. The diffuse brain injury is associated with global disruption of brain tissue usually and is invisible. The focal injuries consist of epidural hematomas (EDH), subdural hematomas (SDH), intracerebral hematomas (ICH), and contusions (coup and contre-coup). The diffuse injuries consist of brain swelling, concussion, and diffuse axonal injury (DAI)<sup>17</sup>.

### **1.5.1 Focal Injury**

Focal injuries result from direct loading and can often occur without widespread, or diffuse, damage. Focal injuries are typically induced when an object penetrates the skull or vertebral column as a result of a motor vehicle accident, gunshot wound, or a blow<sup>18</sup>. As a result, macroscopically visible damage is typically visible at the site of impact, and the clinical symptoms are often very specific to the area that is directly injured. Focal injuries to the brain include epidural hematomas and skull fracture (with or without brain damage). When there is dural compromise, this is often termed open head injury in the clinical setting.

Contact loading can also result in coup (at the site of impact) and contra-coup (away from the site of impact) contusions to the brain, involving both cellular and vascular components. Focal injuries account for one-half of all severe head injuries, but two-third of all deaths in this group.

Spinal cord injury (SCI) is another severe type of injury and is most commonly caused by fracture and dislocation of the spinal column, resulting in a focal injury. The mechanical impact can cause displacement of key components such as bone fragments; inter-vertebral discs, or ligaments, resulting in transient compression or contusion of spinal cord tissue. Spinal cord is compressed at the site of impact that causes the surrounding tissue to lengthen in the longitudinal direction. Tissue near the center of the spinal cord is most vulnerable to damage, suggesting that the mechanical loads are highest in this anatomical region. As in TBI, the nature (whether the impact is stationary/transient), magnitude, and duration of the biomechanical insult can dictate the injury response and may affect functional outcome. Slow stretching of the spinal cord results in very little tissue damage. In fact, increasing the length of the spinal cord up to twice the original length results in very little damage if the elongation is applied slowly. However, rapid application of biomechanical inputs for longer durations (more than 20–30 min) may surpass tissue thresholds and can result in irreversible damage.

#### 1.5.1.1. Subdural Hematoma(SDH)

The most common mechanism of subdural hematoma is tearing of veins that bridge the subdural space as they go from the brain surface to the various dural sinuses<sup>19</sup>.

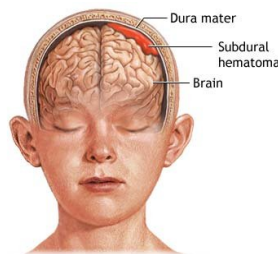


**Figure 1-3: Biomechanics of Subdural hematoma<sup>20</sup>**

### 1.5.1.2. Epidural Hematoma(EDH)

Epidural hematoma is a relatively infrequently occurring sequel to head trauma. It occurs as a result of trauma to the skull and the under laying meningeal vessels and is not due to brain injury<sup>21</sup>.

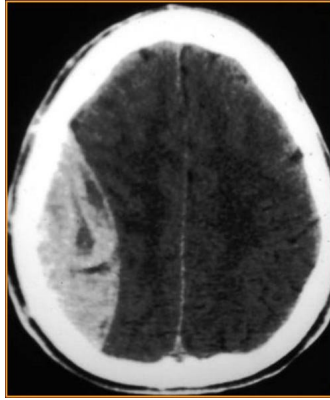


Figure 1-4: CT of Epidural Hematoma<sup>22</sup>

### 1.5.1.3. Intracerebral Hematoma (ICH)

Intracerebral hematomas are well defined, homogeneous collections of blood within the cerebral parenchyma. They are most commonly resulted from sudden acceleration and deceleration of head. Other causes are penetrating wounds and blows to the head.

### 1.5.1.4. Contusion

Cerebral contusion is the most frequently found lesion resulting from head injury. It consists of heterogeneous areas of necrosis, pulping, infarction, hemorrhage and edema.

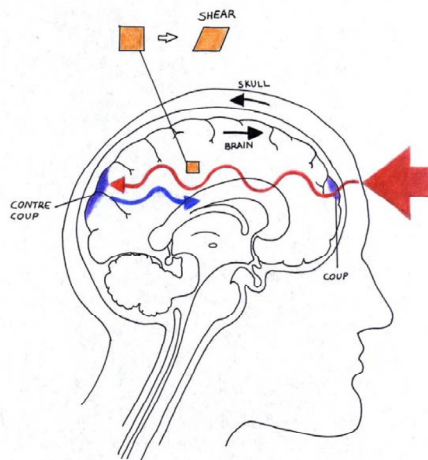


Figure 1-5: Biomechanics of Contusion<sup>23</sup>

Contusions generally occur at the site of impact (defined as coup contusions) and at remote sites from the impact (defined as contre-coup contusions). The contre-coup lesions are more significant than coup-lesions.

### **1.5.2 Diffuse Injury**

Diffuse injuries are most often caused by inertial loading, which describes the motion of objects. The acceleration (rate of change of velocity) is a key parameter in determining tissue response under diffuse injury. Higher accelerations correspond to higher forces (Force equals mass times acceleration, Newton's second law). Because of the complex nature of head-neck dynamics, the brain can be subjected to acceleration when subjected to an external load and therefore TBI often manifests as a diffuse injury. When the acceleration is translational, injuries tend to be localized to a smaller area. However, in the case of rotational acceleration, on the other hand, large magnitude of strains deep within the brain is possible, resulting in diffuse axonal injury (DAI). Most injuries that are observed clinically are a combination of translational and rotational accelerations (referred to as angular acceleration). Diffuse injuries are thought to occur as a result of combination of acceleration and deceleration portions of loading, creating very fast moving, uneven load distributions. Diffuse strains can lead to differential movement of the skull relative to the brain, causing para-sagittal bridging vein injury, as well as intracerebral hemorrhage.

#### **1.5.2.1. Concussion**

The classical cerebral concussion is the most common head injury diagnosis, and it involves immediate loss of consciousness following injury. In general, 95 % of the patients have good recovery at the end of 1 month. More than 99% of the patients are discharged from hospital within 14 days<sup>24</sup>.

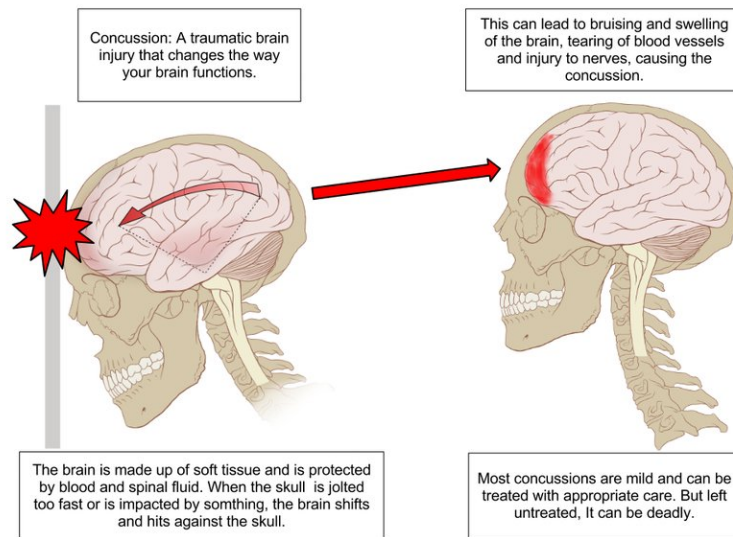


Figure 1-6: Biomechanics of Concussion<sup>25</sup>

#### 1.5.2.2. Diffuse Axonal Injury

Diffuse axonal injury (DAI) is linked with mechanical disruption of many axons in the cerebral hemispheres and sub cortical white matter. Microscopic examination of the brain reveals axonal tearing that occurs throughout the white matter of right and left cerebral hemispheres. In addition, it also involves degeneration of long white matter tracts extending into the brain stem. High-resolution CT scans may show small hemorrhages and axonal swelling occurred during injury. DAI involves immediate loss of consciousness lasting for days to weeks. Severe memory and motor deficits is observed to be present in patients with DAI and post traumatic amnesia can last for weeks. The extent of DAI injury plays a key role in the resulting state after the injury. Patients with severe DAI become unconscious immediately after the injury and either remain comatose or go into a persistent vegetative state. In severe TBI, DAI is compounded due to the presence of widespread vascular injury and traumatic lesions which cause cerebral edema<sup>26 27</sup>.

Diffuse injury to brain can result in widespread dysfunction, therefore making these injuries the most prevalent cause of persistent neurological disability. Clinically, diffuse injury is often observed in closed head injury and arises most often from motor vehicle accidents. The brain is coupled to the skull viscously via the surrounding cerebral spinal fluid (CSF). During normal activity, the CSF protects the brain by viscous dampening of the brain motion, so that impact with skull is prevented. However, this dampening is insufficient for a

sufficiently large external force associated with a rapid deceleration, and the brain will crash against the skull wall, resulting in brain deformation. Different manifestations of TBI result from this brain deformation. Because there is a much lower threshold force required to injure the brain compared to the skull, skull fracture need not always accompany physical brain damage and the resulting head injury is termed “closed”<sup>28 29</sup>.



# Chapter 2

## Model Development

The MRI data for generation of the human head was obtained from the Siemens healthcare of USA, based on their website. The MATLAB image processing software was used for image segmentation. The ANSYS finite element analysis software was used to construct the solid model using B-splines, which read all the coordinates obtained. The models were analyzed, considering various boundary conditions at the neck part. Static analysis and dynamic analysis, using automatic time integration technique, were carried out on these models, for different time steps and for different material properties.

### 2.1 Introduction to MRI

Magnetic resonance imaging (MRI) of the brain is a safe and painless test that uses a magnetic field and radio waves to produce detailed images of the brain and the brain stem. An MRI differs from a CAT scan (also called a CT scan or a computed axial tomography scan) because it does not use radiation<sup>30 31</sup>. During the exam, radio waves manipulate the magnetic position of the atoms of the body, which are picked up by a powerful antenna and sent to a computer. The computer performs millions of calculations, resulting in clear, cross-sectional black and white images of the body. The images are then processed into 3D pictures of the scanned area. This method avoids pinpoint problems in the brain and the brain stem when the scan focuses on those areas. MRI is useful in detecting a variety of vulnerable conditions of the brain such as cysts, tumors, bleeding, swelling, developmental and structural abnormalities, infections, inflammatory conditions, or vascular problems. In addition, MRI of the brain can be useful in detecting certain chronic diseases of the nervous system, such as multiple sclerosis. In some cases, MRI can provide clear images of parts of the brain that can't be obtained as well with an X-ray, CAT scan, or ultrasound. This makes it particularly useful for diagnosing problems with the pituitary gland and brain stem<sup>32</sup>. MRIs are safe and relatively easy. No health risks are associated with the magnetic field or radio waves, since the low-energy radio waves use no radiation. The procedure can be repeated without side effects<sup>33</sup>.

## 2.2 Image Processing in MATLAB

Edge detection of MRI image is carried out using MATLAB image processing. Edge detection is an image processing technique for finding the boundaries of objects within images. It works by detecting discontinuities in brightness. Image Edge detection significantly reduces the amount of data and filters out useless information, while preserving the important structural properties in an image. Canny filter is used to detect edges from the human head MRI<sup>34</sup>.

### Canny edge detectors:

1. Filter image with derivative of Gaussian
2. Find magnitude and orientation of gradient
4. Linking and threshold (hysteresis):
  - Define two thresholds: low and high
  - Use the high threshold to start edge curves and the low threshold to continue them.

MATLAB: `edge (image, 'canny', threshold);`



**Figure 2-1: MRI<sup>10</sup> and Edge detected signal using MATLAB**

Detected edge coordinates were plotted in ANSYS and joined by B-spline method to create the 2-D geometry of human head consisting of 3 main parts: Skull, Cerebrospinal fluid and central nervous system. CNS includes cerebrum (including white and gray matter),

cerebellum, brain stem and spinal cord. Figure 2-2 represents the line model drawn in ANSYS using B-spline and the arrow indicates the different point of loading analysis.

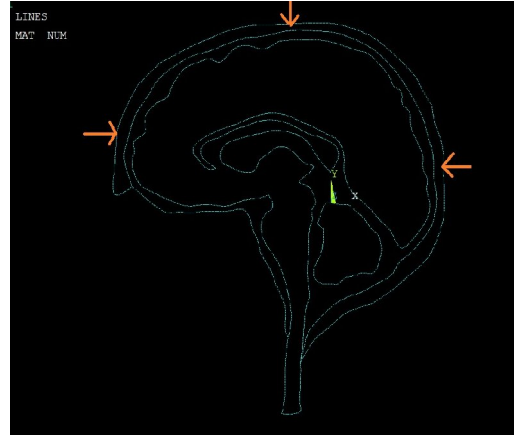


**Figure 2-2: Line Model drawn using B-spline with loading directions**

### **2.3 Finite Element Model Generation**

The biomechanics of the human head can be seen as a brain movement within an externally loaded skull and this gives a complex two and three dimensional dynamic boundary value problem. The internal biomechanical responses of the brain cannot be completely measured by experimental techniques. Analytical models are limited to problems with regular geometry, simple boundary conditions and homogeneous material properties. Numerical approaches, on the other hand, give approximate the analytical solution with a numerical procedure. In Finite element method (FEM), the geometrically complex material domains of the problem can be represented by a collection of geometrically simple sub domains called Finite Elements. The approximation functions are then derived over each finite element, since any continuous function can be represented by a linear combination of algebraic polynomials. In other words, this method can be perceived as a piece wise application of the variational methods, in which the approximation functions are algebraic polynomials<sup>35</sup>.

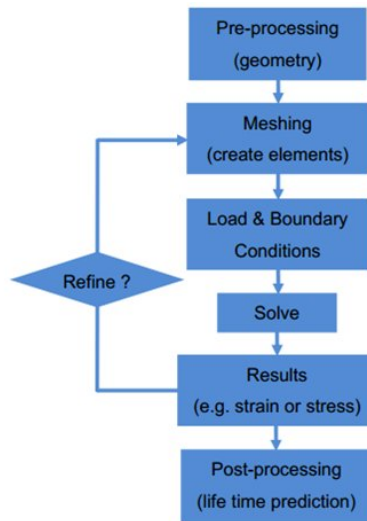


**Figure 2-3: Flow Chart of Finite Element Modeling<sup>36</sup>**

Head injuries are related to tissue material failure, characterized in some form of stress, strain or deformation. Finite element analysis can provide stress, strain or deformation distributions across, and within the different tissues for a given biomechanical input, such as a head motion or head impact. Finite element models are repeatable and reproducible, and simulations can be seen as surrogate experiments without biological variability. In addition, they can also include irregular geometry, inhomogeneous and nonlinear material properties and complex boundary and loading conditions. FEM has been in use for the last 30 years as an engineering tool in various mechanical design processes. In biomechanical field, numerical techniques were first employed to complement experimental car crash simulations. Today, the numerical technique has reached such a level that complex structures like the human being can be modeled with good accuracy. However, significant research remains to be performed before a complete model of the human being can be presented.

### **2.3.1 Mesh Generation and Optimization**

Model generation usually takes on the narrower meaning of generating the nodes and elements that represents the spatial coordinates and connectivity of the actual system. This means that, the model generation is the process of defining the geometric configuration of the model's nodes and elements. Accurate geometrical reconstruction is dictated by the

mathematical solution, especially in 2D or 3D problems, solved by computer simulations. There are two ways of describing geometrical description of the model – parametric and triangular. First approach operates with the 3D parametric spline curves, surfaces and volumes which approximates required real object. This is known as Solid Modeling (SM) approach. In contrast, the second method operates with the points, straight lines, and triangular surfaces. It is called the Direct Mesh Generation (DMG) method. With using DMG it is not possible to change the model during the solution without recreating full model from the very beginning. Parametric approach is much more preferable as the model, reconstructed in this form, is more accurate, contains more information about the object, and could be easily used in any field of analysis.

Plane 183 is used in the present work. Plane 183 is a higher order 2-D, 8-node or 6-node element depicted in Figure 2-4. Plane183 has quadratic displacement behavior and is well suited for modeling irregular meshes. This element is defined by 8 nodes or 6-nodes, having two degrees of freedom at each node: translations in the nodal X and Y directions. The element may be used as a plane element (plane stress, plane strain and generalized plane strain) or as an axisymmetric element. This element can be used for simulating problems involving viscoelasticity, creep, stress stiffening, large deflection and large strain. Furthermore, the above-mentioned element also has mixed formulation capability for simulating deformations of nearly incompressible elasto-plastic materials and fully incompressible hyper elastic materials.

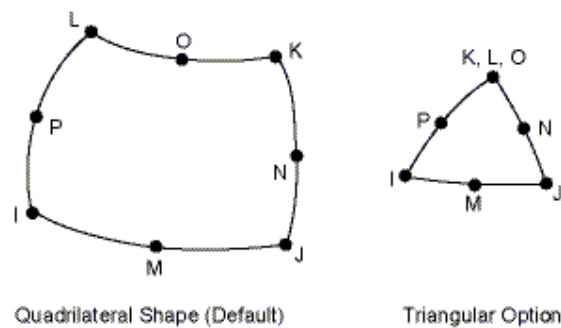


**Figure 2-4: Plane 183 node element<sup>37</sup>**

The selection of element type in the present simulation depended upon the geometry of the component parts in the 2D model. Using quadrilateral mesh made the simulation faster and

precise. Mesh optimization was performed by simulating the problem using different mesh density, so that the results are insensitive to mesh size and number. No change in results was observed while choosing the elements more than 106160. Figures 2-5, 2-6, 2-7 and 2-8 shows how the mesh density affects results:

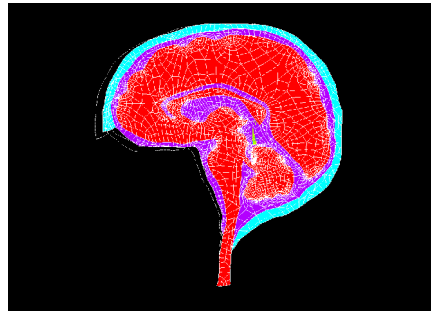


**Figure 2-5: Displacement with No. of elements 3642**

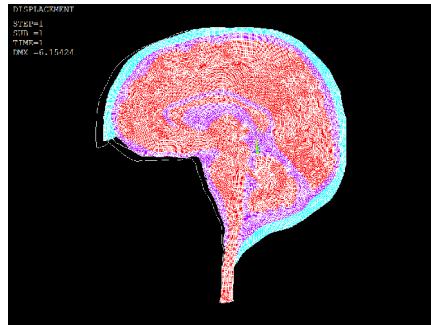


**Figure 2-6: Displacement with No. of elements 33272**

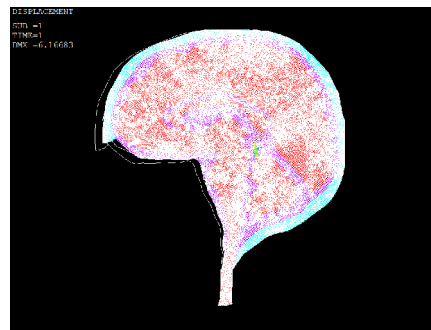


**Figure 2-7: Displacement with No. of elements 106169**



**Figure 2-8: Displacement with No. of elements 205411**

From the above figures one can observe that while increasing the elements no. to more than nearly 100000 displacement results obtained were independent of mesh size and number. Thus, we used mesh density of 205411 for simulations in the present study.

## **2.4 Material Properties**

In practical, most biological tissues have long been recognized as inhomogeneous, anisotropic and nonlinear; however, the complete material characterization of biological tissues is still a daunting task. Hence, meaningful assumptions of material behavior need to be made for the sake of FE model development. The material data for different component parts of the model used in this study are obtained from the literature<sup>38</sup>.

### **2.4.1 Skull**

The human skull consists of a combination of high density (cortical) and low density (cancellous) structures. Bones in general are considered to be anisotropic with many of them having a mineral orientation in the direction of maximum load. Each bone has therefore directional properties according to its unique function. In this study, the three layer cranial bone is modeled as a single-layer structure exhibiting transverse isotropic properties. Skull bone has anisotropic material properties with fiber patterns radially oriented from the center of ossification. This means that the bone stiffness varies in response to force applied from different directions as opposed to isotropic material where the stiffness is the same for all directions<sup>39</sup>.

Transverse isotropic property of skull:

The representation of bone stiffness matrix contains nine components as it has three perpendicular symmetry planes with the principal axis directions going axial, radial, and tangential (circumferential). Bone can be modeled as being orthotropic, but can be often simplified even further by assuming that it has a symmetry plane perpendicular to the fiber direction, making skull to be considered as transversely isotropic. This reduces the parameters required from nine, for orthotropic material, to five. For skull bone, it has been established that the elastic modulus parallel and perpendicular to the fiber direction is not the same. It is also known that the fiber direction is radially directed from the center of ossification. This effectively means that the plane of the axial axis, representing the bone thickness, and the tangential axis is the plane of isotropy. Some parameters of the skull bones cannot be obtained from literature and need to be estimated. The Elastic modulus parameters  $E_1$ ,  $E_2$  and Poisson ratio  $\nu_{12}$  are obtained from literature. The Poisson's ratio  $\nu_{21}$  is calculated using equation (2.1)<sup>9</sup>. Shear modulus for an in-plane orthotropic material could be predicted by equation (2.2)<sup>9</sup>.

$$\frac{\nu_{12}}{E_1} = \frac{\nu_{21}}{E_2} \dots\dots\dots (2.1)$$

$$G_{12} = \frac{\sqrt{E_1 E_2}}{2(1 + \sqrt{\nu_{21} \nu_{12}})} \dots\dots\dots (2.2)$$

where the matrix of Elastic modulus is represented as<sup>9</sup>;

$$E = \begin{bmatrix} \frac{E_1}{1 - \nu_{12}\nu_{21}} & \frac{\nu_{12}E_2}{1 - \nu_{12}\nu_{21}} & 0 \\ \frac{\nu_{12}E_1}{1 - \nu_{12}\nu_{21}} & \frac{E_2}{1 - \nu_{12}\nu_{21}} & 0 \\ 0 & 0 & \frac{E_1}{2(1 + \nu_{12})} \end{bmatrix} \dots\dots\dots (2.3)$$



where,  $E_i$  is the directional Elastic modulus and  $\nu_{ij}$  represents the corresponding Poisson ratios. In a patient specific model, it is important to have accurate parameters in order to obtain reliable results. Obtaining correct parameters can be a hard task and much estimation needs to be done when there is limited data available either from material testing or from literature. Parameters needed for FEM simulation, to study the skulls biomechanical effects during an impact are obtained from literature and estimations. The biomechanical properties, elastic modulus, Poisson's ratio and shear modulus are needed for the skull. The elastic modulus is a measure of the elastic deformation of the material when load is applied to it. It can be obtained from the slope of a stress-strain curve for each material. The shear modulus measures the resistance of a material to shear deformation. Higher value means that the material is more rigid to shear. The shear modulus is defined as the ratio of shear stress versus shear strain. The Poisson's ratio is the ratio of lateral versus longitudinal strain in uniaxial tension. The value is dimensionless and ranges from -1 to 0.5 for stable materials and is equal to 0.5 for incompressible one. In Figure 2-9, principal axis directions showing radial direction parallel to the fiber direction in infant skull bones, tangential direction perpendicular to the fiber direction and axial direction in the bone thickness.

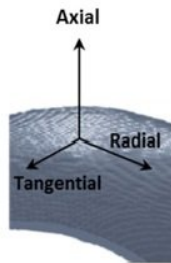


Figure 2-9: Skull bone representation<sup>9</sup>

Table 2-1: Parameters for constitutive model of skull bone<sup>9</sup>

Parameters	Values	Nomenclature
$E_1$	1929MPa	Elastic modulus parallel estimated from linear relation of parallel and perpendicular data.
$E_2$	1092MPa	Elastic modulus perpendicular.

$\nu_{12}$	0.19	Poisson's ratio.
$\nu_{21}$	0.11	Equation (2.1)
$G_{12}$	634.9MPa	Shear modulus in plane of symmetry is estimated using equation (2.2)
Density	2090kg/m <sup>3</sup>	Density
$K$	656.8MPa	Bulk modulus Estimated

### 2.4.2 CSF

The CSF layer representing the entire subarachnoid space is modeled by a homogenized solid material with bulk modulus of 21.9MPa and shear modulus of 50KPa.

The matrix form of elastic modulus for an isotropic elastic material is given as<sup>40</sup> (adapted and re-expressed);

$$\begin{bmatrix} \sigma_{xx} \\ \sigma_{yy} \\ \sigma_{zz} \\ \tau_{xy} \\ \tau_{yz} \\ \tau_{zx} \end{bmatrix} = \begin{bmatrix} E(1-\nu) & E\nu & E\nu & 0 & 0 & 0 \\ E\nu & E(1-\nu) & E\nu & 0 & 0 & 0 \\ E\nu & E\nu & E(1-\nu) & 0 & 0 & 0 \\ 0 & 0 & 0 & G & 0 & 0 \\ 0 & 0 & 0 & 0 & G & 0 \\ 0 & 0 & 0 & 0 & 0 & G \end{bmatrix} \begin{bmatrix} \epsilon_{xx} \\ \epsilon_{yy} \\ \epsilon_{zz} \\ \gamma_{xy} \\ \gamma_{yz} \\ \gamma_{zx} \end{bmatrix} \dots\dots\dots (2.4)$$

where  $E$  is the constant Elastic modulus and  $\nu$  represents the Poisson's ratio.  $\sigma_{ij}$  and  $\tau_{ij}$  represent the normal and shear stress, respectively. The normal and shear strain are represented by  $\epsilon_{ij}$  and  $\gamma_{ij}$ . The above equation represents the stress-strain model for 3D. In the present study, this matrix was scaled down to 2D for computation.

**Table 2-2: Material Properties of CSF** <sup>41</sup>

Parameter	E (Elastic Modulus)	K (Bulk Modulus)	$\nu$ (Poisson's ratio)	Density(kg/m <sup>3</sup> )
CSF	0.15 MPa	21.9 MPa	0.499	1040

### 2.4.3 Brain

During severe impact conditions, brain tissue experiences a rapid and complex deformation, which can be seen as a mixture of compression, tension and shear. More importantly, the deformation can be time dependent too. Diffuse axonal injury (DAI) occurs when both the strains and strain rates exceed 10% and 10/s, respectively<sup>42</sup>. Brain tissue can be considered to behave like a soft gel. Because of the high water content (about 80 %), it is nearly incompressible. Knowing the mechanical properties of brain tissue in shear at these strains and strain rates is thus of particular importance, as they can be used in finite element simulations to predict the occurrence of brain injuries under different impact conditions. Thus, the deformation of brain tissue can be assumed to depend on the shear modulus only. The simplest way to determine the viscoelastic properties of soft biological tissues is to subject the material to periodic oscillations, due to the consistency and problems with load introduction<sup>43</sup>.

Prony series parameters are used to represent the viscoelastic brain properties. In a one dimensional relaxation test, the material is subjected to a sudden strain that is kept constant over the duration of the test, and the stress is measured over time. The initial stress is due to the elastic response of the material. Then the stress relaxes over time due to viscous effect in the material. Typically either a tensile, compressive, Bulk compression, or shear strain is applied. The resulting stress vs. time data can be fitted with no. of equations, called models. Therefore, Prony series for shear relaxation is given as<sup>44</sup>:

$$G(t) = G(\infty) + \sum_{i=1}^n G_i e^{-\left(\frac{t}{\tau_i}\right)} \dots\dots\dots(2.5)$$

where,  $G(\infty)$  = Long term shear modulus.

$1/\tau$  = Decay Constant

$$G(t = 0) = G_0 = G(\infty) + \sum_{i=1}^n G_i \dots\dots\dots(2.6)$$

$G_0$  = Short term shear modulus.

Therefore,  $G(t) = 1 - \sum_{i=1}^n g_i \left( 1 - e^{-\left(\frac{t}{\tau_i}\right)} \right)$  .....(2.7)

where,  $g_i$  = relaxation coefficient;  $\tau_i$  = characteristic relaxation time

The viscoelastic properties for brain are given as:

**Table 2-3: Material properties for CNS**<sup>39</sup>

Parameter	Density(kg/m <sup>3</sup> )	Bulk Modulus(GPa)	Short term shear modulus(kPa)	Long term shear modulus(kPa)	Decay constant(s <sup>-1</sup> )
Brain	1040	2.19	34	6.4	400

Same viscoelastic properties are used for cerebellum, brain stem and spinal cord in this model. Prony series parameters estimated by using above values of long term shear modulus, short term shear modulus and decay constant are:

$$g_1 = 0.5837, \tau_1 = 0.02571s; g_2 = 0.2387; \tau_2 = 0.0257s$$

### 2.5 Boundary Conditions

As for the boundary condition at the head-neck junction, two extreme assumptions i.e., free and fixed boundary conditions can be considered. Most 2D finite element head models in the literature consider the free boundary condition only with the supporting argument being that the neck constraint has negligible influence on the dynamic response of the head model in a short time interval<sup>45</sup>. However, the head model subjected to frontal impact without any constraint at the neck will undergo predominantly rectilinear motion which is not always the case. Therefore, for the case of static loading, we consider a fixed boundary condition, in which the nodes around an area of the spinal cord/brain stem are fully constrained. For dynamic impact simulations, we considered different boundary conditions for different loading directions. For the case of frontal and back impact loading, perpendicular displacement (Y direction) and rotational displacement of nodes around spinal cord/brain stem region were assumed to be zero. Similarly for the case of top loading, X directional displacement and rotational displacement of nodes around spinal cord/brain stem were assumed to be zero. This is illustrated in Figure 3-6 in Chapter 3.

# Chapter 3

## Results and Discussion

Two broad categories of impacts can be defined as static and dynamic loading, with dynamic loading being the most common. The mechanical response to impact is the tissue deformation or strain and will initiate the ensuing pathological events. The impact parameters and the mechanical response will dictate the types of injury (focal and/or diffuse). In the present study, we focus on two categories of impacts, the mechanical response to traumatic impact, and the types of injuries produced. Loads are described as direct (e.g., physical contact between the head and another object) or indirect (e.g., as the result of motion of the head). We simulated the model with direct loading. The type of force and the direction, or plane, of loading, will also affect the resulting mechanical response in the tissue. Impact loading can be either focal or diffuse, depending on the magnitude of the force and area of impact. A traumatic insult to brain or spinal cord will lead to a mechanical response of the tissue that is dependent on the mode (type of impact), severity (correlated with amplitude of static/dynamic force), and anatomical location of the impact as well as the mechanical properties of the tissue. The mechanical properties of a tissue vary from individual to individual, as well as with age and previous injuries or disease. Because of the properties of soft tissues such as brain and spinal cord/brain stem, both the rate and the duration of the impact will also influence the response. The rate of application of loads strongly affects tissue damage due to the viscoelastic material properties of CNS tissue. The tissue deformation is time dependent and is affected by duration and nature (pattern of load cycle in the case of transient loading) of the impact. When loads are applied at a high rate, the tissue cannot absorb (or reduce) the force fast enough and this results in both structural and functional tissue failure. In contrast, slowly applied loads give the tissue “time” to reduce the force and generally result in less damage.

Simulation of an impact to the frontal, top and back region of the head was carried out in ANSYS with goal to compute the shear stress/strain distribution, strain-time history, max

shear stress with respect to frequency and loading criteria for various injuries during dynamic loading condition.

### 3.1 Static Loading

Static loading is a case of very slowly applied direct load. Usually there are no deficits until there is substantial tissue deformation. These loading conditions are relatively rare and often occur in human entrapment situations (e.g., earthquakes).

#### 3.1.1 Frontal Loading

Figure 3-1 depicts the region where frontal loading is applied in the brain model. We considered zero displacement at spinal cord of the model in either direction shown in Figure 3-2.



Figure 3-1: Frontal Loading Point

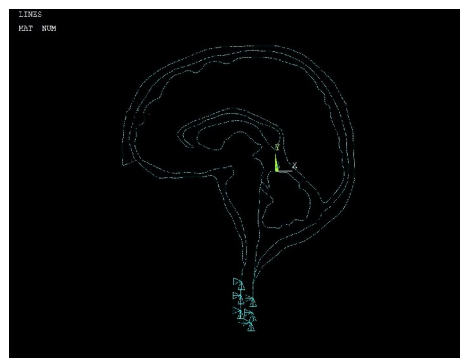
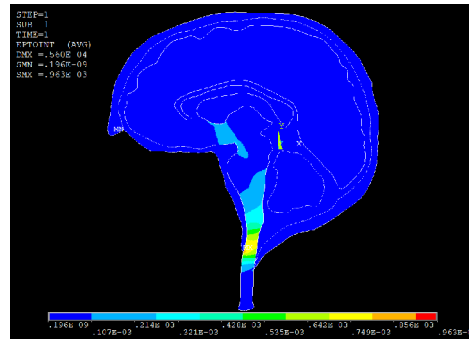


Figure 3-2: Boundary condition for static load

**Point Load = 20N**



**Figure 3-3: Shear strain contour for point load**

**Distributed Load = 20 Pa**

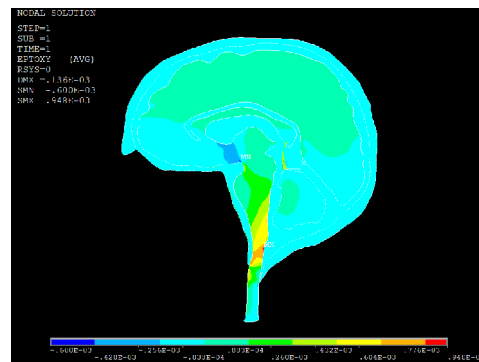


**Figure 3-4: Shear strain contour for distributed load**

From the above simulation, it can be observed that the strain distribution in the case of point loading is confined to the portion of brain stem and spinal cord and rarely extends into areas of cerebrum. However, in the case of distributed loading, the strain is distributed all along the cerebrum and brain stem areas, which even extends to the rear areas of cerebrum. This indicates the significance of distributed loading as compared to point loading. This concludes that the distributed force can damage brain to a large extent than point loading. However, it must also be stated that the magnitude of strain in the areas of brain are significantly smaller compared to strain in brain stem/spinal cord areas. This effectively means, that the magnitude of distributed load is very significant, in order to result in a significant difference in injury compared to point load.

On the other hand, simulations for the case of top loading (Figures 3-6 and 3-7) shows areas of significant strain distribution in localized areas of brain.

### 3.1.2 Top Loading

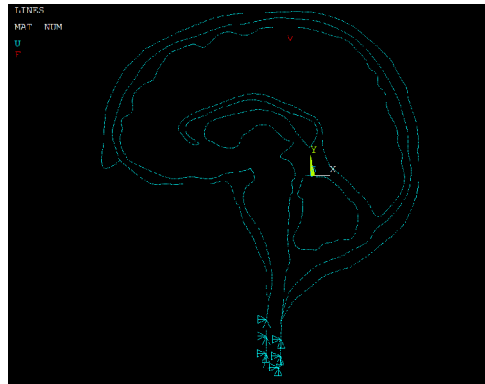


Figure 3-5: Top Loading Point

Point load: 20N

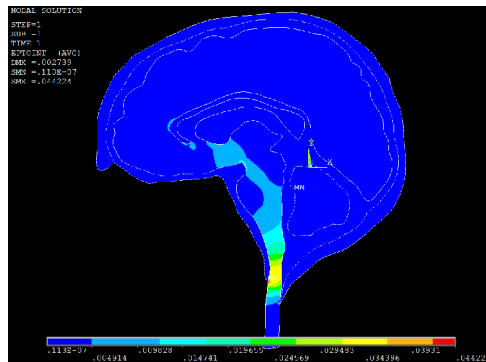


Figure 3-6: Shear strain contour for top point load

Distributed load: 20 Pa

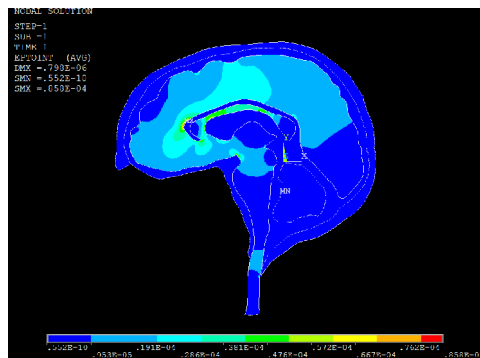
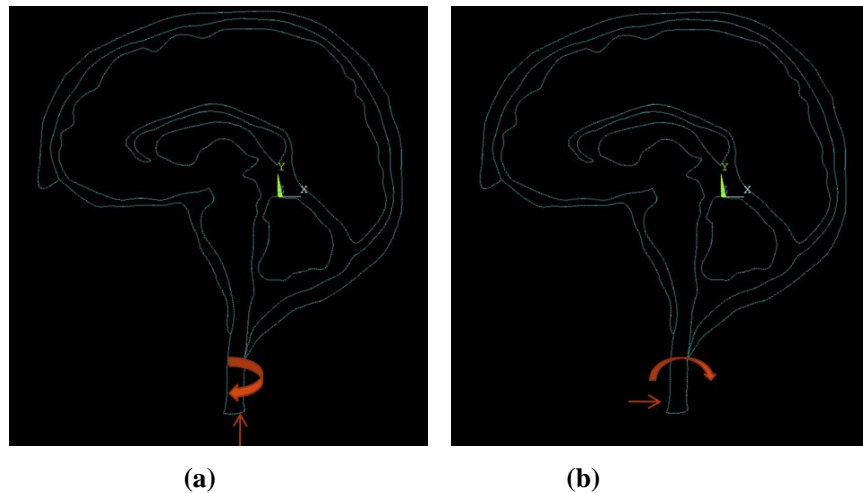


Figure 3-7: Shear strain contour for top distributed load



### 3.2 Dynamic Loading

Dynamic loading can occur quite rapidly (under 1 s, often 50 ms) and is the most common cause of TBI and SCI (spinal cord injury). The present section illustrates three different head injury simulations concerning a frontal, top and back head injury resulting from a time dependent load. In the frontal case, validation is established with available experimental results. Attention is focused on shear stress-time history, maximum shear stress with respect to frequency and related brain tissue damage. We simulated the model with a sinusoidal impact condition of different frequencies. Figure 3-7 depicts boundary conditions used for dynamic simulation. The colored symbols denote the corresponding translational and rotational displacement to be zero, which is applied on the nodes at the lower boundary line of brain stem/spinal cord region.



**Figure 3-8: Boundary condition for Dynamic (a) Frontal and Back loading (Displacement and rotation along Y direction is zero) (b) Top loading (Displacement and rotation along X direction is zero)**

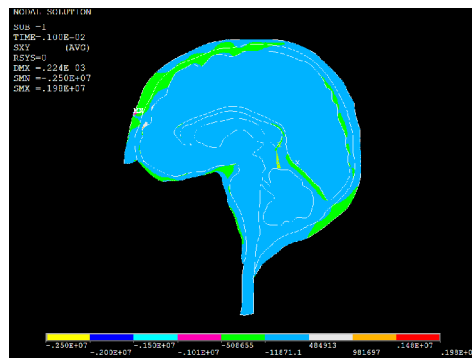
#### 3.2.1 Frontal Loading

The model is simulated by applying a frontal impact described by sinusoidal wave of magnitude of 7kN and frequency of 100Hz.

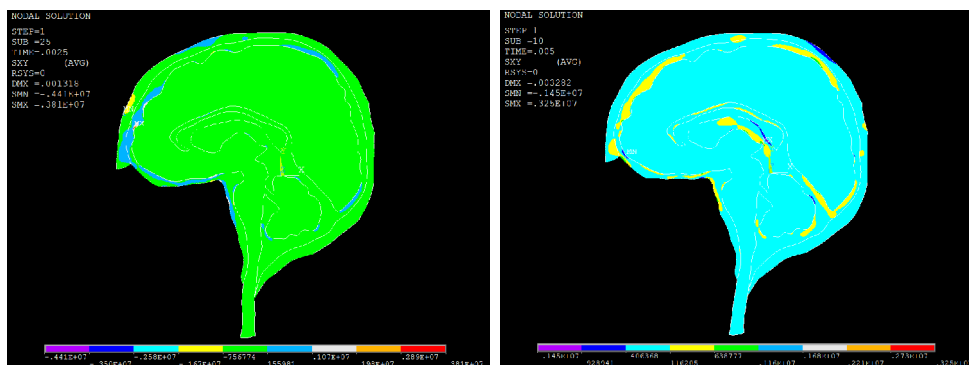
$$F = 7000 * \sin(2 * \pi * f * t)$$

Figure 3-9 shows the predicted shear stress contour changes with time. Contour plot presented are at 2.5ms i.e. at peak of input force wave, at 5ms i.e. the end of first half cycle, at 10ms i.e. at the end of the first cycle, and randomly at 15ms, 30ms, 32.5ms and 50ms. When the head was subjected to the sinusoidal impact resulting in a forward rotation, high

shear stresses on the sagittal plane were concentrated at the occipital area. Maximum shear stress with a magnitude of 1980 kPa first developed at the frontal lobe at 1 ms then exceeded up to 3810 kPa at 2.5 ms. From the shear stress-time history we can see that for the above pulse max shear stress of compressive type occurs at 2.5 ms at frontal region in first cycle. In the third cycle it occurs at 32.5 ms i.e. at the third peak of the input force. At the same time contre-coup pressure of tensile type can also be observed i.e. negative pressure. After 2.5 ms stress at the frontal region starts dropping while at posterior region it starts increasing towards positive values in first cycle. When stress wave reflects back from posterior region it spreads towards parietal lobe that can be observed in the contour plot after 10 ms. Negative pressure (tensile stress) can cause the development of brain cavitation bubbles. After 10ms, coup pressure becomes negative and both negative coup and contre coup pressure can generate severe shock waves which may cause contusion and DAI. At the end of every pulse i.e. at 10ms, for first pulse and 30ms for third pulse maximum shear stress value become very small.



t= 1ms



t=2.5ms

t=5ms

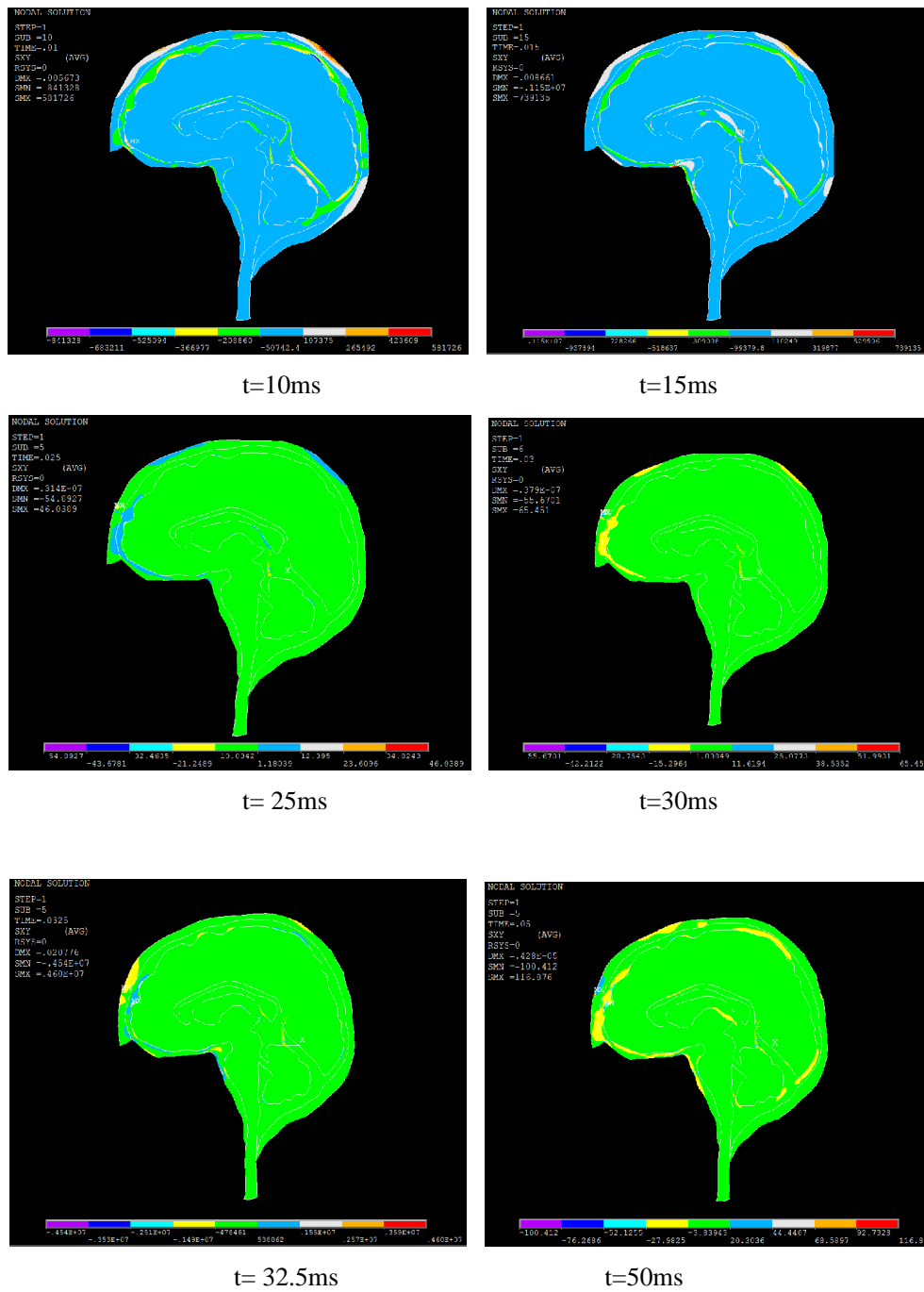


**Figure 3-9: Dynamic frontal loading - Shear stress contours**

This very high shear stress of value 3810 kPa is observed may be because of such high input force of 7000N. As represented in Figures 3-10 and 3-11, plot pattern in coup and contre-

coup site depicts the variations in stress amplitude and coup stress reverse in amplitude after a time period. In addition, the amplitude of coup pressure is more than contre-coup pressure. At the end of first cycle (at 10ms) coup pressure becomes negative, means tensile. Contre-coup stress is already negative and this causes severe cavitations in coup and contre coup site due tensile pressure in both coup and contre coup regions. The traveling stress wave reflects against the skull at the contre-coup site and then moves back towards interior side. This is then followed by a tensile wave (negative pressure wave), which produces irreversible cavitations damage in different brain regions, especially within the contre-coup region, which is also indicated in literature<sup>46</sup>.

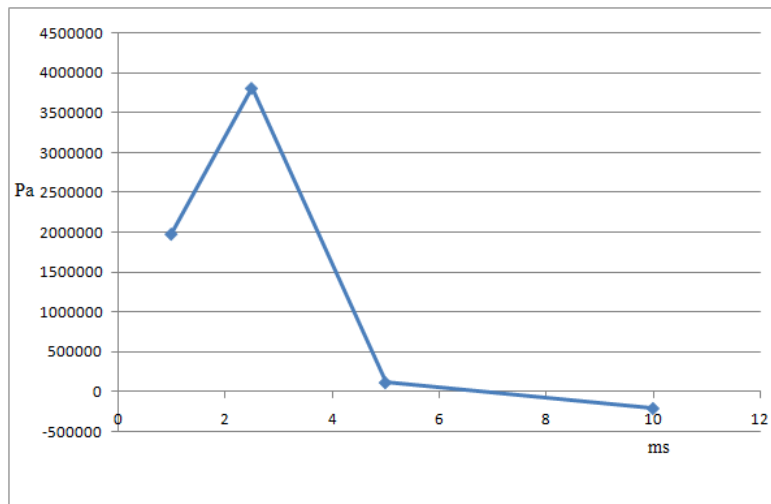


**Figure 3-10: Shear stress at coup site vs. time**

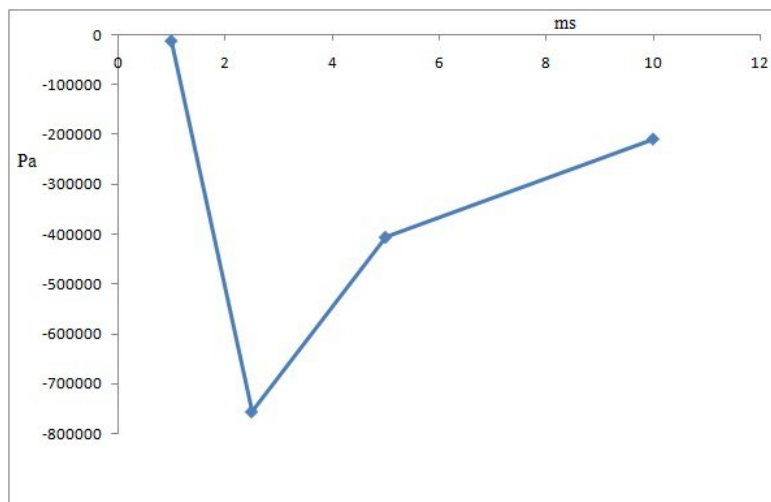


**Figure 3-11: Shear stress at contre-coup site vs. time**

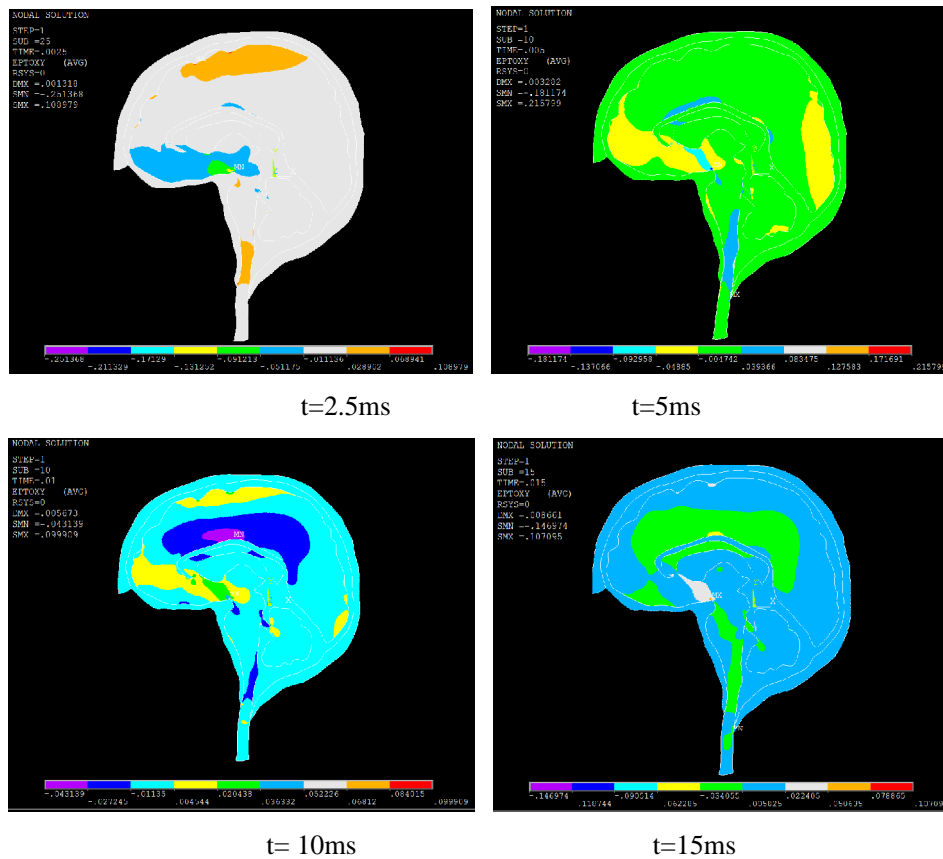
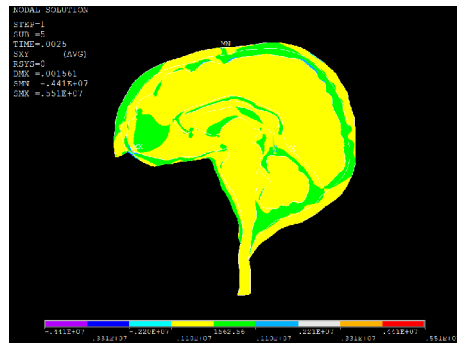


Figure 3-12: Dynamic Frontal loading- shear strain vs. time contours

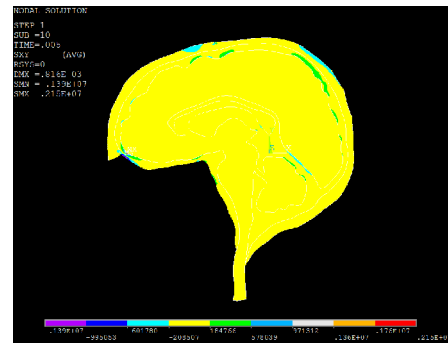
Figure 3-11 represents the shear strain contour profile for the case of frontal loading. In the first half cycle maximum strain can be observed at the vertex of brain stem. After first 5 ms, strain distribution is observed in the complete brain. At 10 ms, negative strain is distributed in the brain which represents the severe axonal damage and cavitations may cause.

### 3.2.2 Top Loading

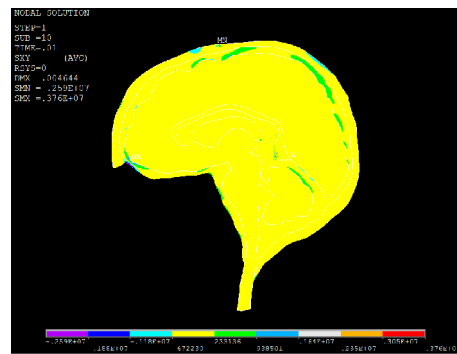
A predictive top impact event was simulated by applying sinusoidal force (as indicated in section 3.2). The simulation resulted in the shear stress and strain profiles depicted in Figures 3-12 and 3-13 respectively. One can observe markedly higher positive and negative stress developed in the coup and contre-coup regions, as compared to the case of frontal impact. Such high shear stresses induce intense and diffused cavitations damage. Again in first cycle at peak of the input force, 2.5 ms maximum shear stress can be observed, which is distributed to the complete brain. After 2.5 ms, stress values decrease and distribution across the brain becomes weaker.



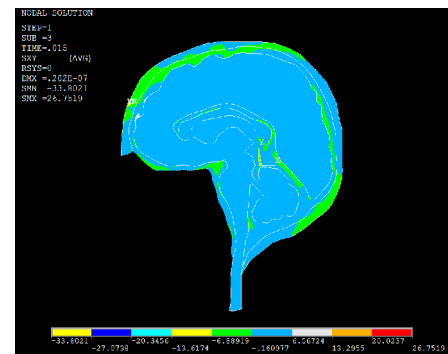
t=2.5ms



t=5ms

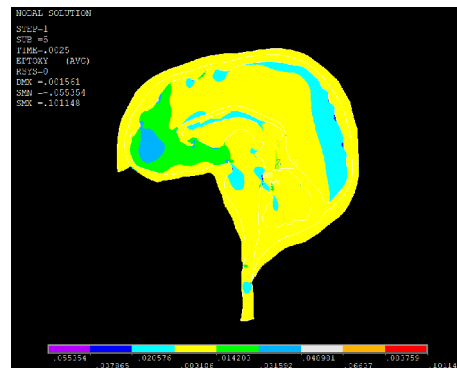


t=10ms

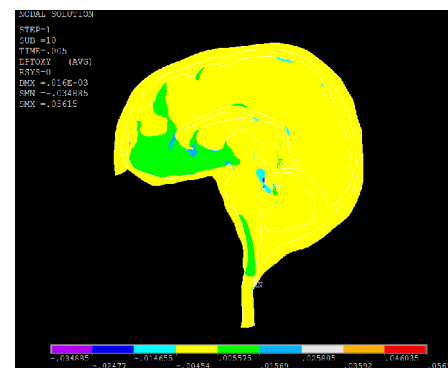


t=15ms

Figure 3-13: Dynamic top loading - shear stress vs. time contours



t=2.5ms



t=5ms

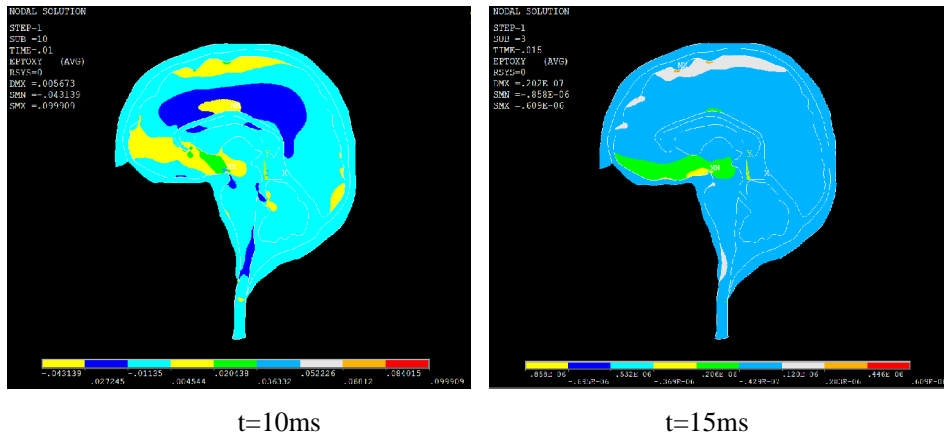
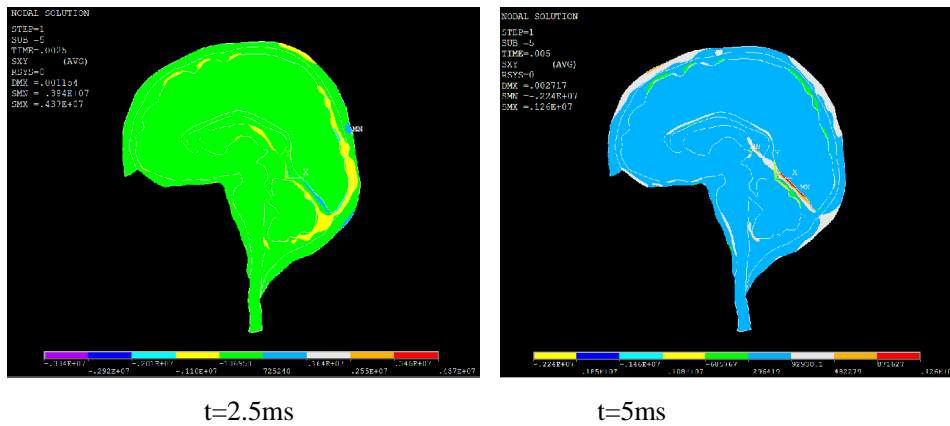
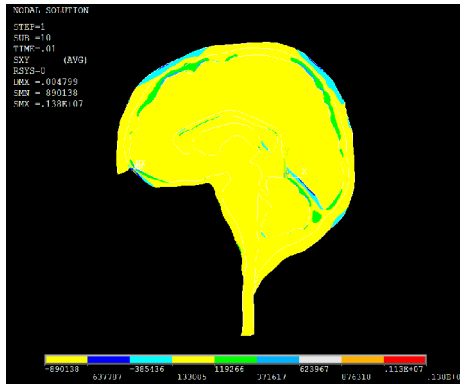


Figure 3-14: Dynamic top loading - shear strain vs. time contours

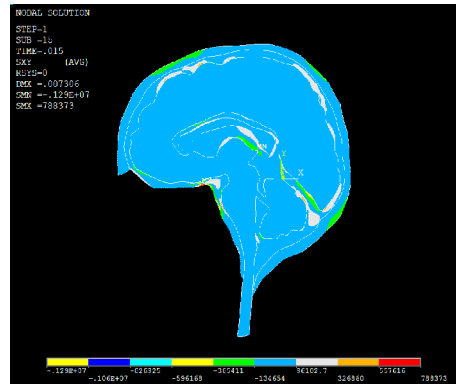
### 3.2.3 Back Loading

For, the prediction of the back impact similar loading condition as described for frontal and top loading is applied at the back key point as in the case of frontal impact. The figure 3-14 and 3-15 represents the shear stress and strain contours variation with time respectively. One can observe that the maximum shear stress is obtained at the peak input force value i.e. at 2.5 ms. Maximum stress obtained in back loading case is much higher than in case of frontal loading. This means back loading may cause more severe injury compared to frontal and top with same impact. The stress distributed to parietal lobe and to the complete brain, in the case of back impact.



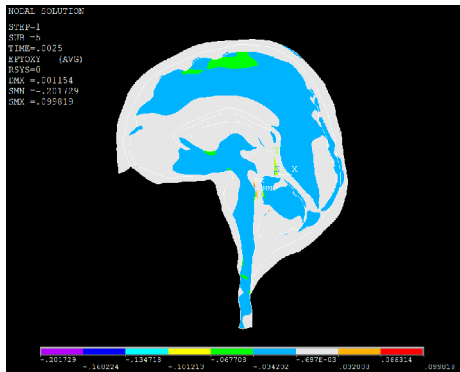


t=10ms

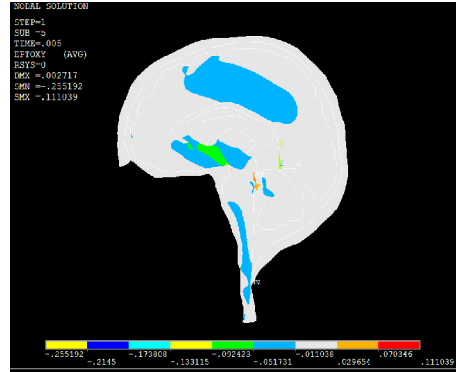


t=15ms

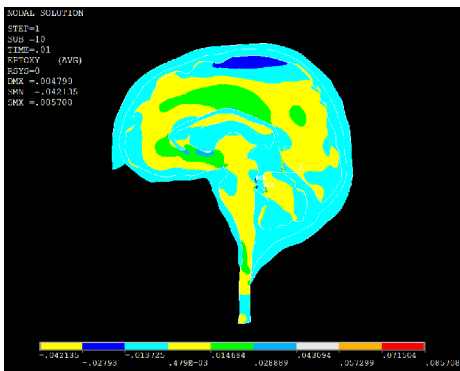
Figure 3-15: Dynamic back loading - Shear stress vs. time contours



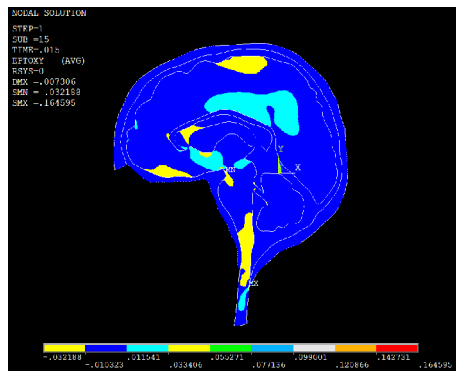
t=2.5ms



t=5ms

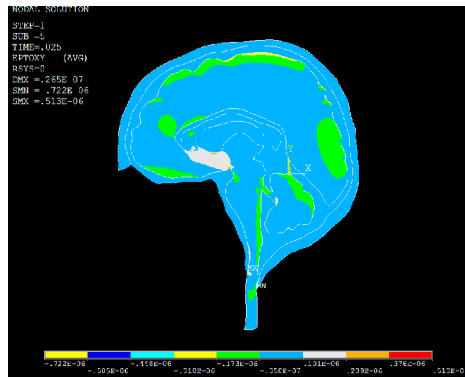


t=10ms



t=15ms





t=25ms

**Figure 3-16: Dynamic back loading - Shear strain vs. time contours**

Mechanically induced brain deformation at a particular region or site as a consequence of applied loading may determine a particular type of brain injury. We observed that a high shear strain was generated at the brain stem when a sagittal section of the human skull, was subjected to a point impact. Brain stem is one region to experience high concentration of shear strain. The structure of brain stem itself resembles a narrow bridge. Therefore, it is highly likely that a high stress/strain concentration can develop in this area of head. For the different cases simulated, areas of high shear strains were initially confined in the cortical region of the brain. Thereafter, the strain distribution propagated to the central core areas of brain, after the impact reached its peak. Moreover, the stress distribution was sensitive to the point of impact, indicating back impact to produce more damage. The development of a highly localized shear strain can probably be explained in the light of structural and anatomic features of midbrain. Midbrain regions act as neural relay stations and are responsible for several vital functions of human body. Hence, higher magnitudes of shear stress in these areas can be responsible for brain dysfunction if the level is sufficiently high to surpass tissue thresholds. The severity of such brain dysfunction could be as extreme as DAI when shear stress/strain experienced by brain tissues exceeds the tissue injury threshold, or as minor as a mild concussion. However, there are multiple factors that limit the present study. Firstly, the exact location and direction of impact is not ascertained, instead key point based loading was performed. In addition, comprehensive knowledge of in vivo material properties of brain tissue is still lacking and research is still required in this direction. The results from the 2D model could still be improved with more accurate representation of brain tissue properties.

# Chapter 4

## Conclusion and Future Work

### 4.1 Conclusion

We have illustrated that clinically relevant injuries, such as DAI and brain cavitation, can be resulted from transient impact on head. Following are the key conclusions from the present study.

1. We simulated the result for static and dynamic load. From that we conclude that dynamic load may cause severe injuries like cavitation and diffuse axonal injury.
2. It is observed that contre - coup injuries can cause serious problems in brain compared to coup injuries.
3. We concluded that, distributed static load causes high strain in brain than point load.
4. In the case of dynamic loading, back impact is more risky than frontal impact in general.
5. The stress waves spreads in the complete brain with time and causes cavitations and axons shearing which can result in diffuse axonal injury.
6. Spinal cord experiences maximum strain in different loading conditions and is the most vulnerable part in static loading.

### 4.2 Future Work

The present work focuses on the 2D representation of injury mechanics of head. Modeling of skull-brain complex and its interface design requires a lot of study of human anatomy as well as mechanical parameters relevant to biological injury in brain. Following are the future works that can be performed following the present model:

1. Failure criteria like von-Misses stress and strain for study of brain injury mechanics can be developed.

2. CSF can be considered as a viscous fluid (to simulate case of CSF leakage upon impact) and skull as completely anisotropic can be simulated.
3. Extraction of meningeal layer from MRI or CT alone is difficult. One can design 3D model with meningeal layers by using the CT and MRI overlapped image.
4. 3D modeling can be performed based on surface generation from MRI images of different section of head region.
5. The effect of medium surrounding head is very important in simulating conditions such as blast loading. Compressible fluid flow simulations will be needed to calculate the impact on head, prior to brain injury modeling.
6. Brain is considered as viscoelastic and these material properties vary with respect to frequency of applied load in transient analysis. Therefore, models could be simulated for different viscoelastic material properties with respect to frequency of applied load in transient analysis.

# References

---

- <sup>1</sup>Nahum, A.M., Smith, R.W., Ward, C.C., Intracranial pressure dynamics during head impact, in: Proceedings of the 21st Stapp Car Crash Conference, 1977.SAE paper no. 770922
- <sup>2</sup> Melvin J., Lighthall W.J., Ueno K. (1993).Accidental injury, biomechanics and prevention. Springer-Verlag, New York Inc. ISBN: 0-387-97881-X.
- <sup>3</sup> Trosseille, X., Tarriere, C., Lavaste, F., et al. (1992). Development of a FEM of the human head according to a specific test protocol. In Proceedings of the 36th Stapp Car Crash Conference, Society of Automotive Engineers, Warrendale, PA, USA.
- <sup>4</sup> Chu C.S and Lee, M.C., Finite element analysis of cerebral contusion. Advances in bioengineering, AMSE-BED-Vol. 20,1991, p.601-604.
- <sup>5</sup> Ruan, J.S, Khalil, T.B, King, A.I., Dynamic response of the human head to impact by three-dimensional finite element analysis, J. Biomech. Engrg. 116 (1994) 44–50.
- <sup>6</sup> Bain, A. C., Billiar, K. L., Shreiber, D. I.,. In vivo mechanical thresholds for traumatic axonal damage. In Proceedings of the Impact Head Injury: Responses, Mechanisms, Tolerance, 1997.
- <sup>7</sup> Al-Bsharat, A., Hardy, W. N., Yang, K., Khalil, T. B., King, A. I., and Tashman, S., Brain/skull relative displacement magnitude due to blunt head impact: new experimental data and model, Proceedings, 43rd Stapp Car Crash Conf.,1997, SAE Paper No. 99S-86.
- <sup>8</sup> Kleiven, S., Biomechanics and thresholds for MTBI in humans. Royal Institute of Technology, School of Technology and Health, PhD Thesis, 2002.
- <sup>9</sup> Oskersdottie, A., Finite Element Analysis of Infant Skull Trauma using CT Images, , Master's thesis, Royal institute of technology,2012.
- <sup>10</sup> <http://www.healthcare.siemens.com/magnetic-resonance-imaging/magnetom-world/toolkit/clinical-images/trio-head>.
- <sup>11</sup> Duane D. Blatter, Erin D. Bigler, Shawn D. Gale, Sterling C. Johnson, MR-Based Brain and Cerebrospinal Fluid Measurement after Traumatic Brain Injury, American Society of Neuroradiology,1996, 18:1–10.
- <sup>12</sup> Prosser,J., P.,John R. Vender,C.,Solares,A., Traumatic Cerebrospinal Fluid Leaks, Elsevier,2011, 857–873.
- <sup>13</sup>Layers covering human brain, Pearson education, 2011.
- <sup>14</sup> Baghaei S.M., Sadegh A.M., Rajaai S.M., An Analytical Model for Investigating the Role of Meningeal Interfaces in the Brain Motion Relative to the Skull in Low-Velocity Head Impacts. International Journal of Biomedical Engineering Technology, 2011, Vol. 5(1), 61–67.
- <sup>15</sup> Engin. A. E. and Wang. H. C. (1970). A mathematical model to determine viscoelastic behavior of in oivo primate brain. J. Biomechanics 3.283-296.
- <sup>16</sup> Anderson C, Bigler E, Blatter D. Frontal lobe lesions, diffuse damage, and neuropsychological functioning in traumatic braininjured patients. J Clin Exp Neuropsychol 1995;17:900–908.

- 
- <sup>17</sup> Bandak F.A, Eppinger R.H, Ommaya A.K. Traumatic Brain Injury: Bioscience and Mechanics. Larchmont, NY: Mary Ann Liebert; 1996.
- <sup>18</sup> Varney, R.N., Roberts, R.J., Forces and Accelerations in Car Accidents and Resultant Brain Injuries,1999,J. Biomech,3004-3208.
- <sup>19</sup> Haines D.E., Harkey H.L., Al-mefty O., The “Subdural” Space: A New Look at an Outdated Concept, Journal of Neurosurgery, 1993, Vol. 32, 111–120.
- <sup>20</sup> <http://m.medlineplus.gov>, David C. Dugdale, University of Washington School of Medicine, Kevin Sheth, University of Maryland School of Medicine, Review provided by VeriMed Healthcare Network, Copyright 1997-2014, A.D.A.M.
- <sup>21</sup> Zimmerman RA, Bilaniuk LT. Computed tomography staging of traumatic epidural bleeding. Radiology 1982;144:809–812.
- <sup>22</sup> [http://en.wikipedia.org/wiki/Epidural\\_hematoma](http://en.wikipedia.org/wiki/Epidural_hematoma)
- <sup>23</sup> Bhateja, A., Shukla, D.,NIMHANS, Banglore, Indian Journal of Neurotrauma(INJT),2009,115 Coup and contrecoup head injuries: Predictors of outcome.
- <sup>24</sup> Evans RW. The post-concussion syndrome. In: Evans RW, Baskin AJNR: 18, January 1997 brain injury 9 DS, Yatsu FM, eds. Prognosis of Neurological Disorders. New York, NY: Oxford University Press; 1992:97–107
- <sup>25</sup> <http://commons.wikimedia.org/wiki>.
- <sup>26</sup> Adams JH, Doyle D, Ford I, Gennarelli TA, Graham DI, McLellan DR. Diffuse axonal injury in head injury: definition, diagnosis, and grading. Histopathology 1989;15:49–59
- <sup>27</sup> Cotter, C.S., Smilarkiewicz, P.K; Szczyrba, I.N., On Mechanisms of Diffuse Axonal Injuries. Bioengineering Conference, ASME 2001. 315-316.
- <sup>28</sup> Zimmerman R.A, Bilaniuk L.T, Genneralli T., Computed tomography of shearing injuries of the white matter. Radiology 1978;127:393–396
- <sup>29</sup> Levin H.S, Meyers C.A, Grossman R.G, Sarwar M. Ventricular enlargement after closed head injury. Arch Neurol 1981;38:623–629
- <sup>30</sup> Gentry L.R, Godersky J.C, Thompson B, Dunn V.D. Prospective comparative study of intermediate-field MR and CT in the evaluation of closed head trauma. AJNR Am J Neuroradiol 1988;9:91–100
- <sup>31</sup> Kelly A.B, Zimmerman R.D, Snow R.B, Gandy S.E, Heier L.A, Deck MD. Head trauma: comparison of MR and CT experience in 100 patients. AJNR Am J Neuroradiol 1988;9:699–708
- <sup>32</sup> Gentry LR, Godersky JC, Thompson B. MR imaging of head trauma: review of the distribution. AJNR Am J Neuroradiol 1988; 9:101–110
- <sup>33</sup> Wilberger JE, Deeb Z, Rothfus W. Magnetic resonance imaging in cases of severe head injury. Neurosurgery 1987;20:571–576
- <sup>34</sup> Solmon, C., Breckon, T., Logan, L.D., Fundamentals of Digital Image Processing using MATLAB, Willey-Blackwell, 2011, 230– 231.

- 
- <sup>35</sup> Maji, W. A., Singh, S., Joldes, G., Washio, T., Chinzei, K., Miller K., Evaluation of Accuracy of Non-Linear Finite Element Computations for Surgical Simulation: Study Using Brain Phantom, *Computer Methods in Biomechanics and Biomedical Engineering*, 2010, Vol. 13(6), 783–794.
- <sup>36</sup> <https://sites.google.com/site/monkology/gpuprogramming-project3-final>.
- <sup>37</sup> Yazdizadeh, B., *Proc. of the Yerevan State Univ. Phys. and Mathem. Sci.*, 2010, No. 3, p. 44–50.
- <sup>38</sup> Yamada, H., ‘Strength of biological materials’. F G Evans. The Williams & Wilkins Company, Baltimore. 1970
- <sup>39</sup> Mcelhaney, J.H., John W., Melvin, Russell R., Haynes, V., Mechanical properties of cranial bone, *J. biomechanics*, 1970.495-511
- <sup>40</sup> Bower A.F., *Applied Mechanics of Solids*, CRC Press, 2011
- <sup>41</sup> Sayed, T.E., Mota, A., Fraternali, F., Ortiz, M., *Biomechanics of traumatic brain injury* J. Elsevier, 2008,4962-4701
- <sup>42</sup> Rashid, B., Destrade, M., Gilchrist, Mechanical characterization of brain tissue in simple shear at dynamic strain rates, *J. Elsevier*, 2013, 28:71-85.
- <sup>43</sup> Miller K., Chinzei K., Mechanical Properties of Brain Tissue in Tension, *Journal of Biomechanics*, 2002, Vol. 30, 1115–1121.
- <sup>44</sup> Mottahedia, M., Dadalaub, A., Haflac, A., Verld, A., Numerical analysis of relaxation test based on Prony series material model, *J. Simtech*, 2010
- <sup>45</sup> Yang, Q., Stainer, L., Ortiz, M., A variational formulation of the coupled thermo-mechanical boundary-value problem for general dissipative solids, *J. Mech. Phys. Solids* 54 (2006) 401–424.
- <sup>46</sup> Brennen, C.E., Cavitation in biological and bioengineering contexts, in: *Fifth International Symposium on Cavitation*, Osaka, Japan, 2003.